Mechanism of Superoxide Ion Disproportionation in Aprotic Solvents

Claude P. Andrieux, Philippe Hapiot, and Jean-Michel Savéant*

Contribution from the Laboratoire d'Electrochimie Moléculaire de l'Université de Paris 7, Unité Associée au CNRS No. 438, 75251 Paris Cedex 05, France. *Received July 31, 1986*

Abstract: The electrochemical reduction of dioxygen in dimethyl sulfoxide is investigated as a function of the addition of acids by means of double potential step chronoamperometry. Analysis of the kinetics as a function of dioxygen and acid concentrations and of the measurement time in a series of acids involving five phenols and nitromethane allowed the determination of the reaction mechanism and of the characteristic rate constants. The $HO_2^{\bullet}$ radical resulting from the neutralization of the initial superoxide anion radical, $O_2^{\bullet-}$, undergoes an electron-transfer reduction by $O_2^{\bullet-}$ itself rather than abstracting a hydrogen atom from the solvent or exchanging an H atom with another $HO_2^{\bullet}$ radical, a commonly accepted mechanism. The mechanism appears to be the same in dimethylformamide, pointing to the conclusion that disproportionation of superoxide ions follows the same reaction pathway in aprotic organic solvents and in water.

In view of its significance in natural and industrial processes, the reduction of dioxygen has been the object of a very large number of studies. Most of the electrochemical investigations in this connection have been carried out in water.[1] The reduction of dioxygen then leads to hydrogen peroxide or water, which implies that the electron-transfer steps are accompanied by homogeneous or heterogeneous chemical steps involving protonations and oxygen–oxygen bond breaking. These chemical reactions are usually so fast that the detection and characterization of intermediates, and thus the establishment of the reaction mechanism, are not possible.

A fruitful approach to this problem has been to use dipolar nonacidic solvents in order to stabilize the first electron transfer intermediate, viz., the superoxide anion radical, similarly to what has been done extensively in aromatic organic electrochemistry.[2] The superoxide anion radical thus produced has been characterized by its cyclic voltammetry reversible wave in various nonaqueous solvents and also by its UV–vis and ESR spectra.[3,4]

The next step was to add Brønsted acids to the aprotic solvent and observe the resulting changes in the reduction signal.[5] It has been shown that the addition of acid converts the reversible one-electron $O_2/O_2^{\bullet-}$ wave into an irreversible two-electron wave featuring the formation of hydrogen peroxide.

$$O_2 + e^- \rightleftarrows O_2^{\bullet-} \quad (1)$$

$$O_2^{\bullet-} + e^- + 2H^+ \rightarrow H_2O_2$$

The exact mechanism of the latter process is, however, not known with certainty. If little doubt is left about the fact that its first step involves the protonation of superoxide anion radicals[5]

$$O_2^{\bullet-} + HA \rightleftarrows HO_2^{\bullet} + A^- \quad (2)$$

several questions remain as to the nature of the successive steps: heterogeneous vs. homogeneous electron transfer; electron vs. H-atom transfer disproportionation; and H-atom transfer from the solvent vs. successive electron and proton transfers?[6] The purpose of work reported hereafter was to answer these questions, using double potential step chronoamperometry, for nonaqueous aprotic solvents. Relatively weak acids (phenol, substituted phenols, nitromethane) were used in order that the dioxygen reduction could be made reversible, at least partially at the lower edge of the time window. Most of the experiments were carried out in dimethyl sulfoxide (Me_2SO).[7] It will be shown that the commonly accepted mechanism involving the H-atom transfer disproportionation of two $HO_2^{\bullet}$ radicals is not followed in Me_2SO.[6] Additional experiments were carried out to check that, as expected from the similarity of the two solvents, the same conclusion holds for dimethylformamide (DMF) in which most of the previous studies were conducted.[6]

The present study thus allowed us to establish what the mechanism of the disproportionation of superoxide ions in aprotic solvents is and to compare it with that in water, an important question in view of the occurrence of this reaction in living organisms.[8]

Results and Discussion

Typical cyclic voltammetry patterns obtained for the reduction of O_2 in Me_2SO upon addition of a weak acid such as a phenol

(1) (a) Bagotskii, V. S.; Nekrasov, L. N.; Shumilova, N. A. *Ups. Khim.* **1965**, *34*, 1697 [*Russ. Chem. Rev. (Engl. Transl.)* **1965**, *34*, 717]. (b) Damjanovic, A. In *Modern Aspect of Electrochemistry*; Conway, B. E., Bockris, J. O. M., Eds.; Butterworths: London, 1969; Vol. 5, p 369. (c) Hoare, J. P. *Encyclopedia of Electrochemistry of the Elements*; Bard, A. J., Ed.; Dekker: New York, 1974; Vol. II, pp 192–382. (d) Appleby, A. J. In *Modern Aspects of Electrochemistry*; Conway, B. E., Bockris, J. O. M., Eds.; Plenum: New York, 1974; Vol. 9, p 369. (e) Wilshire, J.; Sawyer, D. T. *Acc. Chem. Res.* **1979**, *12*, 105. (f) Van den Brink, F.; Barendrecht, E.; Visscher, N. *Recl. Trav. Chim. Pays-Bas* **1980**, *99*, 253. (g) Yeager, E. *Electrochim. Acta* **1984**, *29*, 1527. (h) Sawyer, D. T.; Valentine, J. S. *Acc. Chem. Res.* **1981**, *14*, 393.

(2) Andrieux, C. P.; Savéant, J. M. In *Investigations of Rates and Mechanisms of Reactions*; Bernasconi, C. F., Ed.; Willey: New York, 1986; Vol. 6, 4/E, Part 2, pp 305–390.

(3) (a) Maricle, D. L.; Hodgson, W. G. *Anal. Chem.* **1965**, *37*, 1562. (b) Peover, M. E.; White, B. S. *J. Chem. Soc., Chem. Commun.* **1965**, 183. (c) Peover, M. E.; White, B. S. *Electrochim. Acta* **1966**, *11*, 1061. (d) Sawyer, D. T.; Roberts, J. L. *J. Electroanal. Chem.* **1966**, *12*, 90. (e) Slough, W. *J. Chem. Soc., Chem. Commun.* **1965**, 184. (f) Johnson, E. L.; Pool, K. H.; Hamm, R. E. *Anal. Chem.* **1967**, *39*, 888. (g) Fee, J. A.; Hildenbrand, P. G. *FEBS Lett.* **1974**, *39*, 79. (h) Ozawa, F.; Hanaki, A.; Yamamoto, H. *FEBS Lett.* **1977**, *74*, 99. (i) Sawyer, D. T.; Seo, E. T. *Inorg. Chem.* **1977**, *16*, 499.

(4) (a) This also allowed for the investigation of the reaction of superoxide ions with other electrophiles than water, for example, alkyl[4b,4c] and aryl halides.[4d] (b) Merritt, M. V.; Sawyer, D. T. *J. Org. Chem.* **1970**, *35*, 2157. (c) Dietz, R.; Forno, A. E. J.; Larcombe, B. E.; Peover, M. E. *J. Chem. Soc. B* **1970**, 816. (d) Gareil, M.; Pinson, J.; Savéant, J. M. *Nouv. J. Chim.* **1981**, *5*, 311.

(5) (a) Sawyer, D. T.; Chiericato, G.; Angelis, C. T.; Nanni, E. J.; Tsuchiya, T. *Anal. Chem.* **1982**, *54*, 1720. (b) Chin, D. H.; Chiericato, G.; Nanni, E. J.; Sawyer, D. T. *J. Am. Chem. Soc.* **1982**, *104*, 1296. (c) Roberts, J. L.; Sawyer, D. T. *Isr. J. Chem.* **1983**, *23*, 430. (d) Cofré, P.; Sawyer, D. T. *Anal. Chem.* **1986**, *58*, 1057.

(6) Sawyer et al. favor a mechanism involving H-atom transfer disproportionation of HO_2 radical on the basis of driving force arguments.[5b-d] This mechanism, however, appears questionable as discussed in detail in the following.

(7) (a) The choice of Me_2SO as the solvent was dictated by the result of a related study of the homogeneous catalysis of O_2 reduction by the methylviologen cation radical.[7b] Me_2SO was then used because it is one of the rare organic aprotic solvents able to dissolve methylviologen salts. (b) Andrieux, C. P.; Hapiot, P.; Savéant, J. M. *J. Electroanal. Chem.* **1985**, *189*, 121.

(8) Cass, A. E. G. In *Metalloproteins*; Part I; Harrison, P., Ed.; Verlag Chemie: Weiheim, 1985; pp 121–156.

0002-7863/87/1509-3768$01.50/0

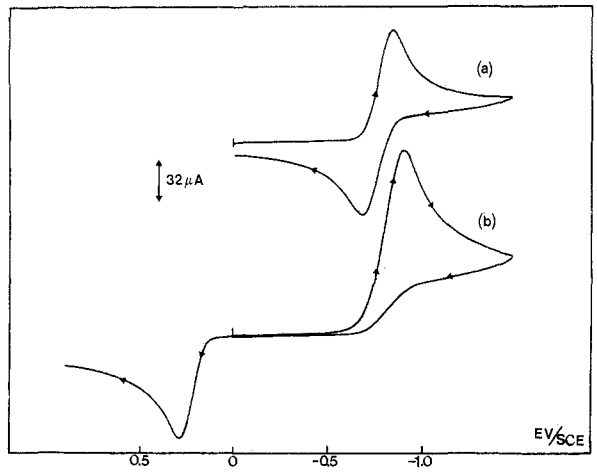

Figure 1. Cyclic voltammetry of dioxygen (2.1 mM) in Me_2SO in the absence (a) and presence (b) of phenol (0.1 mM). $v = 0.2$ V·s^{-1}. Temperature 25 °C.

are shown in Figure 1. The $O_2/O_2^{\bullet-}$ wave loses its reversibility and increases in height, the electron stoichiometry passing from 1e to 2e per molecule. The irreversible anodic wave observed at more positive potentials upon scan reversal features the oxidation of the phenate ions showing, by comparison to an authentic sample, that the overall stoichiometry corresponds to the reaction

$$O_2 + 2e^- + 2HA \rightarrow H_2O_2 + 2A$$

Since the following experiments were carried out in unbuffered media, it was important to be sure that the initial solution did not contain initially the conjugate base of the acid, the presence of which could alter the kinetic response. This was done in each case by checking the absence of the oxidation wave of phenate ions.

Another important point to be checked is that the overall reaction does correspond to the equation writen above without significant side reactions involving the solvent and various possible intermediates. Electrolysis of an oxygen-saturated solution in Me_2SO in the presence of 0.1 M PhOH at the potential of the cyclic voltammetric wave (Figure 1) did show the formation of 95% H_2O_2 after the passage of two electrons per molecule.

For a quantitative investigation of the kinetics, double potential step chronoamperometry (DPSC) was preferred to cyclic voltammetry because the heterogeneous electron transfer to dioxygen in Me_2SO is not very rapid, having a standard rate constant of about 10^{-3} cm·s^{-1}.[3d] The kinetics of electron transfer would thus interfere besides that of the follow-up reactions in the characteristics of the cyclic voltammograms upon raising to sweep rate, rendering the extraction of the kinetics of the follow-up reaction difficult and inaccurate.[2] Provided ohmic drop is appropriately compensated and the potential is stepped at a sufficiently negative value, the use of DPSC is more advantageous since the kinetics of electron transfer does not interfere under these conditions. A time window of 0.002–0.5 s was available in the DPSC experiments. Five phenols and nitromethane, i.e., weak acids (pKs ranging from 15.7 to 17.5), were used. Addition of the acid in increasingly large concentration leads to a progressive decrease of the chemical reversibility of the $O_2/O_2^{\bullet-}$ reduction wave. Typical results are displayed in Figures 2–4 as the variations of the ratio[2,9]

$$R = \left[\frac{i(2\theta)}{i(\theta)}\right] \Big/ \left[\frac{i(2\theta)}{i(\theta)}\right]_{diff}$$

with the experimental parameter θC_{HA}. θ is the inversion time of the double potential step signal, $i(\theta)$ is the cathodic current at the inversion time, and $i(2\theta)$ is the anodic current at twice the

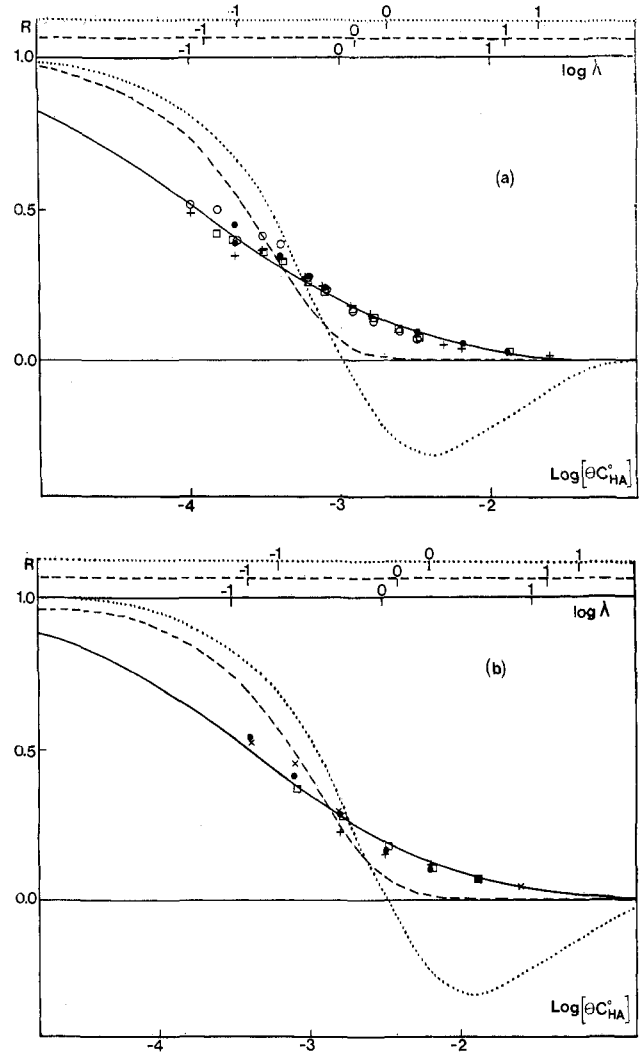

Figure 2. Double potential step chronoamperometry of dioxygen in Me_2SO (+0.1 M NBu_4BF_4) in the presence of (a) *p*-cresol [$C^\circ_{O_2} = 2.1$ mM, $C^\circ_{HA} = 200$ mM (●), 100 mM (+), 50 mM (○); $C^\circ_{O_2} = 0.44$ mM, $C^\circ_{HA} = 50$ mM (□)] and (b) 2,4-dimethylphenol [$C^\circ_{O_2} = 2.1$ mM, $C^\circ_{HA} = 400$ mM (+), 200 mM (□), 100 mM (×), 50 mM (●)]. Working curves: DISP2 (—), DISP1 (- - -), ECE_{irr} (···), same symbolism for the log λ scale corresponding to each working curve. Temperature, 25 °C.

inversion time. The denominator is the same expression as the numerator for a reversible process, i.e., in the absence of acid. In this way, $R \rightarrow 1$ for short times and/or low acid concentrations whereas $R \rightarrow 0$ under converse conditions. C_{HA} is the added acid concentration.

After the formation of $O_2^{\bullet-}$ (reaction 1) and its protonation by the added acid (reaction 2), the resulting $HO_2^\bullet$ radical may undergo various types of reactions:

Reduction at the electrode surface

$$HO_2^\bullet + e^- \rightleftarrows HO_2^- \quad (3)$$

followed by protonation of HO_2^-

$$HO_2^- + HA \rightarrow H_2O_2 + A^- \quad (4)$$

Reactions 1 + 2 + 3 form an ECE (electrochemical–chemical–electrochemical) reaction scheme.[2,10a] According to whether the

(9) Childs, W. V.; Maloy, J. T.; Keszthelyi, C. P.; Bard, A. J. *J. Electrochem. Soc.* **1971**, *118*, 874.

(10) (a) Amatore, C.; Gareil, M.; Savéant, J. M. *J. Electroanal. Chem.* **1983**, *147*, 1. (b) Due to a transcription error, the drawing of the DISP2 working curve in ref 7a is not correct in the upper part of the curve. This has been corrected in the curve shown in Figures 1 and 2.

(11) (a) The occurrence of this type of reaction has not been considered so far. It has, however, been shown that $HO_2^\bullet$ radicals can abstract H atoms from a good donor, 1,4-cyclohexadiene.[11b] (b) Sawyer, D. T.; Roberts, J. L.; Calderwood, T. S.; Sugimoto, H.; McDowell, M. S. *Philos. Trans. R. Soc. London B* **1985**, *311*, 483.

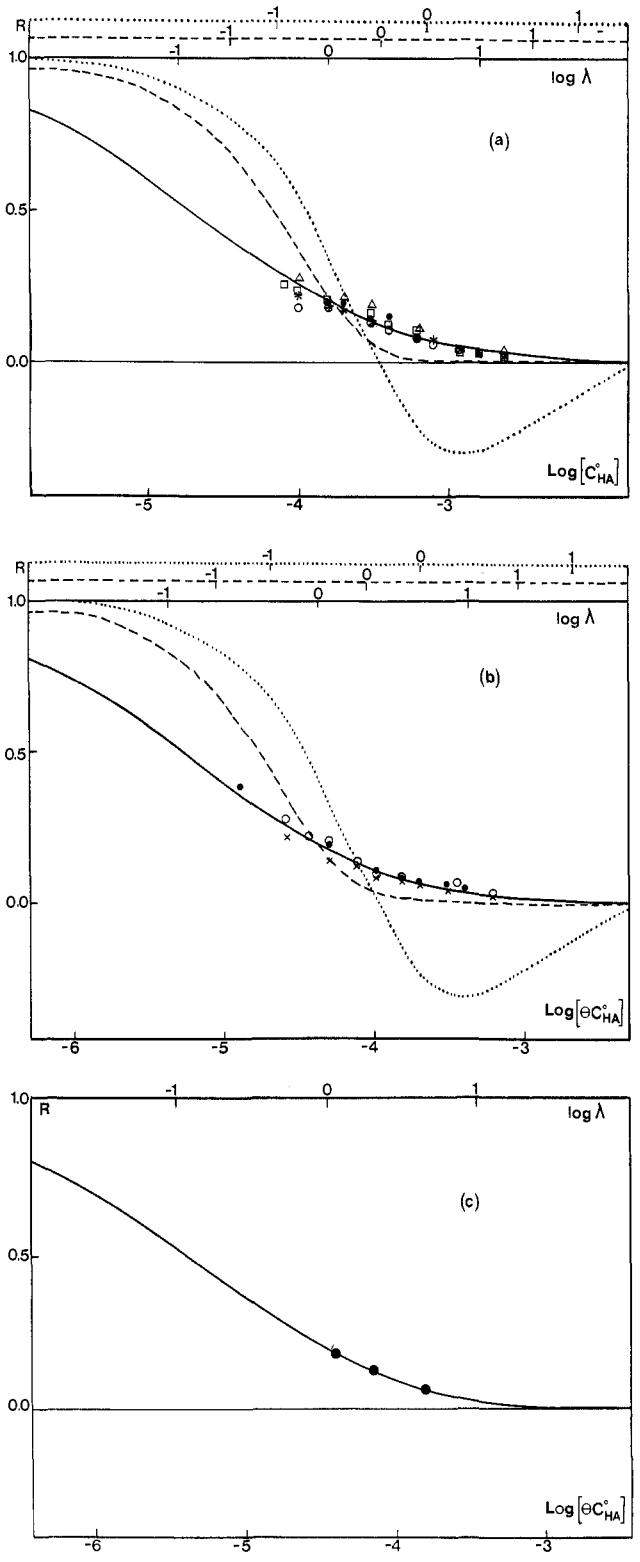

Figure 3. Double potential step chronoamperometry of dioxygen in Me_2SO (+0.1 M NBu_4BF_4) in the presence of (a) phenol [$C°_{O_2}$ = 2.1 mM, $C°_{HA}$ = 100 mM (*), 50 mM (●), 25 mM (□); $C°_{O_2}$ = 0.44 mM, $C°_{HA}$ = 100 mM (△), 50 mM (○)], (b) *p*-chlorophenol [$C°_{O_2}$ = 2.1 mM, $C°_{HA}$ = 50 mM (●), 25 mM (×), 12.5 mM (○)] and (c) *p*-bromophenol [$C°_{O_2}$ = 2.1 mM, $C°_{HA}$ = 10 mM (●)]. Working curves as in Figure 1. Temperature, 25 °C.

protonation reaction 2 is irreversible or reversible, two limiting kinetic behaviors are obtained that we denote ECE_{irr} and ECE_{rev}, respectively.[10a]

Reduction by $O_2^{\cdot-}$ in the solution

$$HO_2^{\cdot} + O_2^{\cdot-} \rightarrow HO_2^- + O_2 \qquad (5)$$

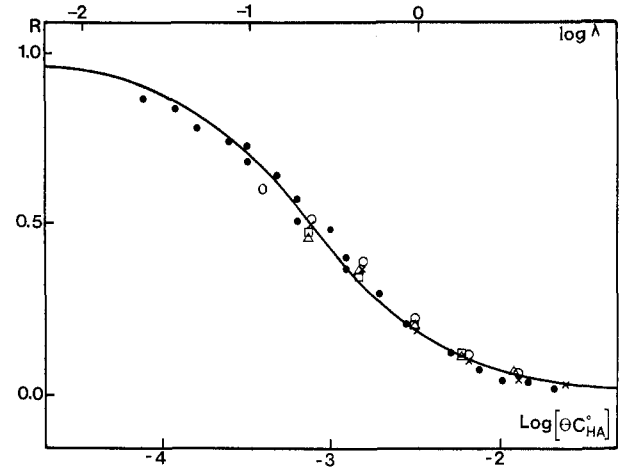

Figure 4. Double potential step chronoamperometry of dioxygen in Me_2SO (+0.1 M NBu_4BF_4) in the presence of nitromethane: $C°_{O_2}$ = 2.1 mM, $C°_{HA}$ = 100 mM (●), 50 mM (×), 20 mM (○); $C°_{O_2}$ = 0.44 mM, $C°_{HA}$ = 42 mM (△), 22 mM (□). Working curve for a mixed DISP1–DISP2 mechanism with k_{-2}/k_5 = 0.5, $\lambda = k_2 C°_{HA}$.

followed by the same protonation step as above. This amounts to an electron transfer disproportionation since $HO_2^{\cdot}$ and $O_2^{\cdot-}$ have formally the same oxidation state. Two limiting behaviors are again obtained depending upon the nature of the rate-determining step. If this is reaction 2, implying that backward reaction 2 is slower than reaction 5, a DISP1 kinetic behavior is obtained.[10a] Conversely, if backward reaction 2 is faster than reaction 5, reaction 2 acts as a preequilibrium vis-ã-vis reaction 5 which is then the rate-determining step. This limiting behavior is denoted DISP2.

H-atom abstraction from the solvent (SH)[11]

$$HO_2^{\cdot} + SH \rightarrow H_2O_2 + S^{\cdot} \qquad (6)$$

In general $S^{\cdot}$ may undergo a variety of further reactions according to the nature of the solvent, to the potential range within which it is generated, and to the basicity of the medium.[12] In the case of Me_2SO, $S^{\cdot}$ appears as very easy to reduce.[12] According to the rate of reaction 2, $S^{\cdot}$ may be reduced at the electrode[12b]

$$S^{\cdot} + e \rightleftarrows S^-$$

or in the solution

$$S^{\cdot} + O_2^{\cdot-} \rightarrow S^- + O_2$$

In all cases S^- is further protonated by HA. In both cases, two subcases are found according to whether the rate-determining step is either forward reaction 2 or reaction 6 with reaction 2 acting as a preequilibrium. We thus obtained four different limiting behaviors that we denote ECE_{irr}, ECE'_{irr}, DISP1, and DISP3, respectively.

H-atom disproportionation

$$2HO_2^{\cdot} \rightarrow H_2O_2 + O_2 \qquad (7)$$

This corresponds to the mechanism proposed by Sawyer et al.[5b-d] According to whether reaction 2 or reaction 7 (with reaction 2 acting as a preequilibrium) is the rate-determining step, two different limiting behaviors are met. In the first case, one obtains the DISP1 behavior, the same as with the preceding reaction schemes. In the second case another limiting behavior is obtained that we denote DISP4.

In all these limiting situations, the current response, under the form of the ratio *R* defined above, is a function of a single dimensionless kinetic parameter, λ, which formally depends upon

(12) (a) M'Halla, F.; Pinson, J.; Savéant, J. M. *J. Electroanal. Chem.* **1978**, *89*, 347. (b) M'Halla, F.; Pinson, J.; Savéant, J. M. *J. Am. Chem. Soc.* **1980**, *102*, 4120. (c) Andrieux, C. P.; Badoz-Lambling, J.; Combellas, C.; Lacombe, D.; Savéant, J. M.; Thiébault, A.; Zann, D. *J. Am. Chem. Soc.* **1987**, *107*, 1518.

Table I. Kinetic Characteristics of the Various Limiting Behavior

limiting[a] behavior	ECE_{rev}	ECE_{irr}	ECE'_{irr}	DISP1	DISP2	DISP3	DISP4
γ^b	−1	0	−1	0	0	−1	−1
δ^b	2	1	1	1	1	1	2
$k_{ap}{}^c$	K_2k_2	k_2	K_2k_6	k_2	K_2k_5	K_2k_6	$K_2{}^2k_7$

[a] For the designation of the limiting mechanisms (see text). [b] Exponents in the dimensionless rate law (see text). [c] Apparent rate constant (see text).

Table II. Fitting of the Experimental Data Obtained with Phenols in Me_2SO and DMF with the Working Curves for the Various Limiting Mechanisms[a]

acid	solvent	ECE_{irr}	DISP1	DISP2
4-chlorophenol	Me_2SO	0.26	0.076	0.019
phenol	Me_2SO	0.256	0.085	0.026
p-cresol	Me_2SO	0.254	0.113	0.026
2,4-dimethylphenol	Me_2SO	0.255	0.099	0.027
phenol	DMF	0.256	0.070	0.021
p-cresol	DMF	0.271	0.097	0.014

[a] As represented by the standard error $\epsilon = [\sum_{i=1}^{N}(R_i^{expt} - R_i^{theor})^2/N]^{1/2}$ (for definition of symbols see text).

Table III. Fitting of the Experimental Data Obtained in Me_2SO upon Varying the O_2 Concentration at a Fixed HA Concentration[a] and the HA Concentration at a Fixed O_2 Concentration[a]

Fixed HA Concentration

acid	DISP2	DISP3	DISP4
phenol (0.05 M)	0.028	0.113	0.065
p-cresol (0.05 M)	0.027	0.111	0.073

fixed O_2 Concentration

acid	O_2 (concn, mM)	DISP2	DISP4
phenol	2.1	0.019	0.040
p-cresol	2.1	0.026	0.056

[a] As represented by the standard error $\epsilon = [\sum_{i=1}^{N}(R_i^{expt} - R_i^{theor})^2/N]^{1/2}$ (for definition of symbols see text).

the switching time, θ, the bulk concentrations of O_2 and HA, $C^\circ_{O_2}$ and C°_{HA}, and an apparent rate constant, k_{ap}, which is a combination of the pertinent rate and equilibrium constants in each reaction scheme.[2,13]

$$\lambda = k_{ap}(C^\circ_{O_2})^\gamma(C^\circ_{HA})^\delta\theta \qquad (I)$$

In each case the $R(\lambda)$ working curve can be obtained from the numerical resolution of the corresponding set of partial derivative equations resulting from the second Fick law modified by the introduction of the appropriate homogeneous kinetic terms. The values of the exponents γ and δ and the expression of k_{ap} for each limiting behavior under unbuffered conditions (as in the experiments we carried out) are summarized in Table I. They were derived from previous studies[10] with the exception of the ECE'_{irr}, DISP3, and DISP4 cases which are analyzed in the Experimental Section. With all six acids, it was found that the current ratio, R, is independent of the dioxygen concentration. Thus, $\gamma = 0$. On the other hand, δ was found equal to 1 from the observation that R remained the same upon varying the acid concentration while keeping the product $C^\circ_{HA}\theta$ constant. This eliminates the ECE_{rev}, DISP3, and DISP4 mechanisms. We thus retain three possibilities—ECE_{irr}, DISP1, and DISP2—in the first stage of the analysis. However, since only two concentrations of oxygen, not very different one from the other, were used, we will come back later on to the question of the incompatibility of the first series of mechanisms with the experimental data. Each of the ECE_{irr}, DISP1, and DISP2 mechanisms is characterized by a particular kinetic parameter λ (see eq I and Table I), and the R vs. log λ working curve differs from one case to the other, allowing the recognition of the actual reaction mechanism (Figures 2 and 3).

For the five phenols, it appears that the DISP2 working curve fits with the experimental data whereas the DISP1 and ECE_{irr} working curves do not. This can be seen in Figures 2 and 3, and in a more quantitative way in Table II. The experimental data were fitted with the working curve in each case by minimizing the standard error

$$\epsilon = [\sum_{i=1}^{N}(R_i^{expt} - R_i^{theor})^2/N]^{1/2}$$

(N is the number of data points, R_i^{expt} is the experimental value of R, and R_i^{theor} is the theoretical value of R for the considered mechanism). The minimal values of ϵ are listed in Table II. It is seen that they are clearly much smaller for the DISP2 mechanism than for the other two mechanisms. The resulting value of the error function ϵ is smaller than ±0.03, a reasonable estimate of the experimental absolute error on R, in the first case and clearly above, ±0.03 for the other two mechanisms. As seen in Figure 3, the number of points obtained in the case of 4-bromophenol is too limited, owing to the fastness of the protonation reaction, to carry out a meaningful mechanism analysis. In this case, we assumed that the same mechanism as with the other phenols is followed in order to estimate the rate characteristics (see below). In order to test the sensitivity of the fitting technique to the changes in O_2 concentration in the limited range where it could be varied, the DISP3 and DISP4 mechanisms were tested as reported in Table III. The results show that the standard error function, ϵ, is much larger than with the DISP2 mechanism and significantly bigger than the experimental absolute error. This clearly points to the conclusion that the absence of variation of the kinetics with O_2 concentration is meaningful even though it was varied in a rather narrow range. A confirmation that the DISP4 mechanism should be rejected comes from the effect of the concentration of

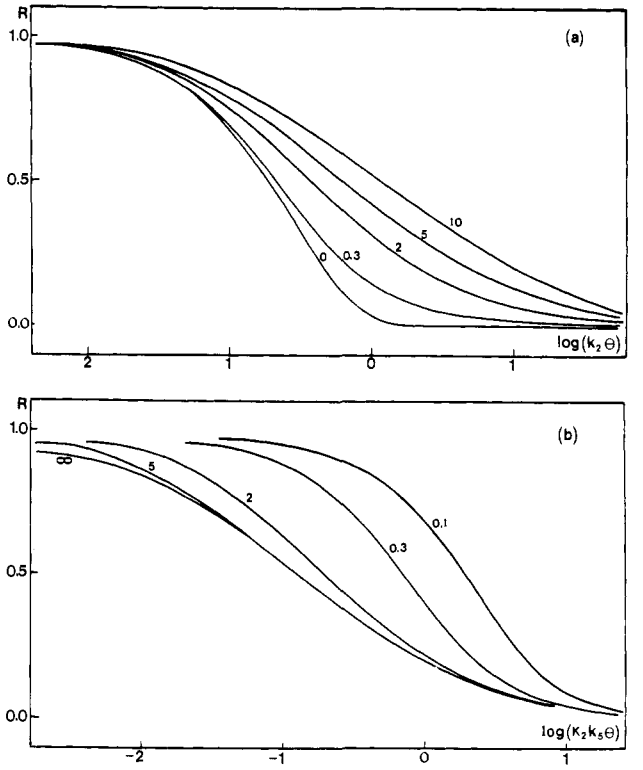

Figure 5. Variations of the DPSC R ratio with $k_2\theta$ (a) or $K_2k_5\theta$ (b) as a function of the competition parameter k_{-2}/k_5.

(13) (a) Amatore, C.; Savéant, J. M. *J. Electroanal. Chem.* **1978**, *86*, 227. (b) Amatore, C.; Savéant, J. M. *Ibid.* **1980**, *107*, 353. (c) Amatore, C.; Gareil, M.; Savéant, J. M. *J. Electroanal. Chem.* **1984**, *176*, 377.

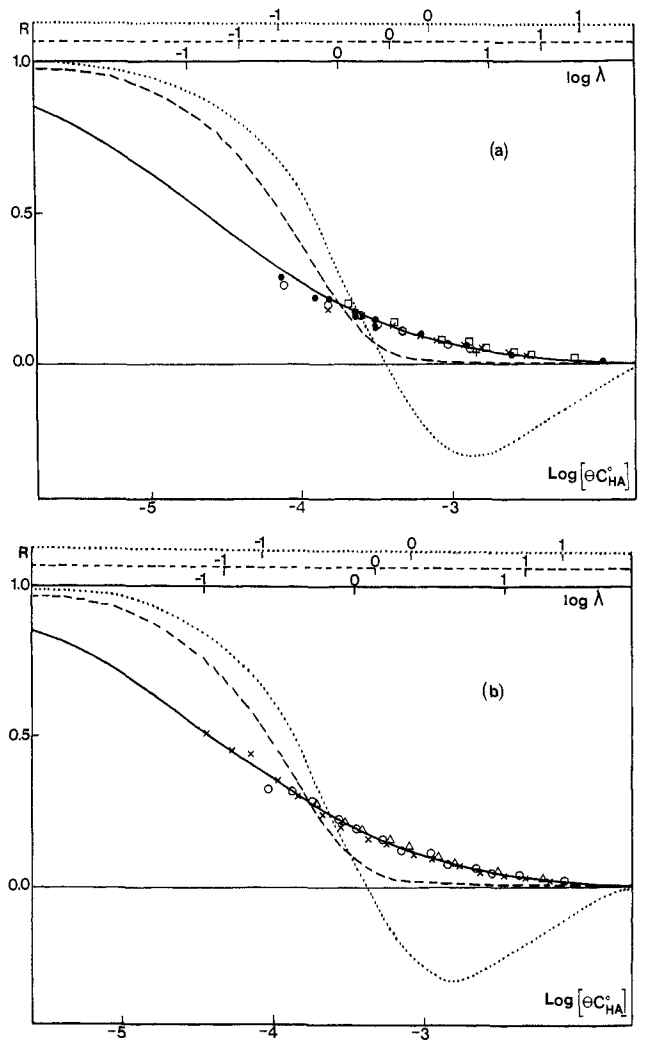

Figure 6. Double potential step chronoamperometry of dioxygen in DMF (+0.1 NBu_4BF_4) in the presence of (a) phenol [$C°_{O_2}$ = 4.8 mM, $C°_{HA}$ = 18 mM (●), $C°_{HA}$ = 46 mM (+); $C°_{O_2}$ = 1 mM, $C°_{HA}$ = 18 mM (○), $C°_{HA}$ = 46 mM (×), $C°_{HA}$ = 100 mM (□)] and (b) *p*-cresol [$C°_{O_2}$ = 1 mM, $C°_{HA}$ = 18 mM (×), $C°_{HA}$ = 46 mM (○), $C°_{HA}$ = 100 mM (△)]. Working curves: DISP2 (—), DISP1 (---), ECE_{irr} (···); same symbolism for the log λ scale corresponding to each working curve. Temperature, 25 °C.

acid, at a given O_2 concentration, since the predicted value of δ is 2 with DISP4 instead of 1 with DISP2. The results displayed in Table III again clearly show that the experimental data fit with the DISP2 mechanism and not with the DISP4 mechanism. A first conclusion is thus that the reduction of dioxygen in the presence of phenols in Me_2SO follows the mechanism consisting of reactions 1 + 2 + 5 + 4 with reaction 2 acting as a preequilibrium vis-à-vis the rate-determining step (reaction 5).

From a chemical point of view, it thus appears that the $HO_2^•$ radicals formed upon protonation by any of the five phenols investigated here in Me_2SO undergo predominantly a further electron transfer from the superoxide anion radical rather than abstracting an H atom from the solvent or disproportionating along an H-atom exchange reaction.[6] The fact that the second electron transfer takes place in the solution rather than at the electrode surface (ECE process) is not surprizing. The very fact that we have been able to observe the fate of $O_2^{•-}$ using DPSC implies that its lifetime is larger than about 1 ms. Thus, the $HO_2^•$ radicals are formed at a rather large distance from the electrode surface and cannot diffuse back to the electrode without reacting with $O_2^{•-}$ radicals diffusing in the opposite direction. This problem has previously been analyzed quantitatively and the same conclusion reached in the case of the reduction of aromatic molecules, such as anthracene and naphthalene in aprotic solvents.[10,13]

Table IV. Fitting of the Experimental Data Obtained with Nitromethane in Me_2SO with the Working Curves for the DISP1–DISP2 Mechanism[a]

DISP1	DISP1–DISP2 with k_{-2}/k_5				DISP2
(k_{-2}/k_5 = 0)	0.1	0.3	0.5	1.0	(k_{-2}/k_5 = ∞)
0.067	0.046	0.033	0.029	0.033	0.065

[a] As represented by the standard error $\epsilon = [\sum_{i=1}^{N}(R_i^{expl} - R_i^{theor})^2/N]^{1/2}$ (for definition of symbols see text).

The results obtained with nitromethane in Me_2SO (Figure 4), although leading to the same chemical conclusions, are somewhat different. Again, the kinetics does not depend upon O_2 concentration, allowing for the elimination of the ECE_{rev}, ECE'_{irr}, DISP3, and DISP4 mechanisms. The ECE_{irr} should also be eliminated for the same reasons as above. The kinetics then appear to fall in between the DISP2 and DISP1 behaviors. As shown in the Experimental Section, the ratio R then depends upon two parameters that can be chosen alternatively as either $k_2C°_{HA}\theta$ and k_{-2}/k_5 or $K_2k_5C°_{HA}\theta$ and k_{-2}/k_5. When the later is large, i.e., backward reaction 2 is fasther than reaction 5, DISP2 predominates and vice versa. The R vs. $k_2C°_{HA}\theta$ or R vs. $K_2k_5C°_{HA}\theta$ working curves can be obtained for any value of the competition parameter k_{-2}/k_5 (Figure 5).

A good fit of the data points can be obtained for k_{-2}/k_5 = 0.5 (Figure 4) as derived from the minimization of the standard error, ϵ, as a function of the two kinetic parameters (Table IV). It is thus again concluded that the predominating reaction is, as in the case of phenols, the electron transfer disproportionation of $HO_2^•$ and $O_2^{•-}$ radicals. The kinetic control is, however, no longer by the homogeneous electron transfer step alone. It jointly involves the protonation of the $O_2^{•-}$ radical.

As indicated earlier,[6] Sawyer et al. concluded from a stop-flow study of the disproportionation of electrogenerated $O_2^{•-}$ radicals upon addition of weak acids in DMF and from driving force arguments that the predominating mechanism involves the H-atom transfer disproportionation of two $HO_2^•$ at variance with what we find in Me_2SO. This is surprising in view of the fact that the two solvents have very similar acid–base properties. We thus undertook to check that the electron transfer disproportionation mechanism we found in Me_2SO is also followed in DMF. Two phenols, phenol itself and *p*-cresol, were investigated in this purpose along the same lines as in Me_2SO. The results are displayed in Figure 6 and Table II. They show without ambiguity that the mechanism of disproportionation involves, as in Me_2SO, a homogeneous electron transfer between $O_2^{•-}$ and $HO_2^•$ taking place in the context of a DISP2 kinetics and not an H-atom exchange between two $HO_2^•$ radicals.[14] Fitting the data points with the appropriate working curve, DISP2 in the case of phenols,

(14) It was concluded from stop-flow experiments in DMF[5b] that the kinetics of disappearance of $O_2^{•-}$ upon addition of phenols is first order in phenol and does not depend upon the initial $O_2^{•-}$ concentration. The formal kinetics of the homogeneous counterpart of the electrochemical DISP1–DISP2 mechanism

$$2\left(\frac{1}{y} - 1\right) + \left(2 - \frac{k_5}{k_{-2}}\right)Lny = K_2k_5C°_{HA}t \quad (y = C_{O_2^{•-}}/C°_{O_2^{•-}})$$

does not depend upon $C_{O_2^{•-}}$ either. It is difficult to see if such a law could fit with the experimental data in ref 5b because of the uncertainty of the initial conditions: the zero-time UV–visible absorption of $O_2^{•-}$ is not the same for all phenols and decreases very significantly as the phenol becomes more and more acidic. Furthermore, if a first-order (DISP1-like) behavior is actually observed under the conditions of the stop-flow experiments, it indicates that the protonation reaction 2 is rate determining and says nothing about the following steps. It does not therefore allow a conclusion of whether disproportionation involves homogeneous electron transfer (reaction 5) or H-atom disproportionation (reaction 7). The latter reaction was thought to predominate on the basis of driving force arguments[5b-d] that we will discuss later on.

(15) (a) Chantooni, M. K.; Kolthoff, I. M. *J. Phys. Chem.* **1976**, *80*, 1306. (b) Courtot-Coupez, J.; Le Dêmêzet, M. *Bull. Soc. Chim. Fr.* **1969**, 1033. (c) Bordwell, F. G. *Pure Appl. Chem.* **1977**, *49*, 963. (d) *Handbook of Chemistry and Physics*; 61st ed.; Weast, R. C., Ed.; CRC Press: Boca Raton, 1980; pp 165–166. (e) Kieffer, F.; Rumpf, P. *C. R. Acad. Sci. Paris* **1954**, *238*, 700. (f) Sawyer, D. T. *Oxygen and Oxy-Radicals in Chemistry and Biology*; Powers, E. J., Rodgers, M. A. J., Eds.; Academic Press: New York, 1981.

Table V. Electrochemical Reduction of Dioxygen in Me_2SO and DMF in the Presence of Acids. Thermodynamic and Kinetic Characteristics[a]

acid	pK_A^{HA}	log K_2k_5	$pK_A^{HO_2\cdot/O_2\cdot^-}$ + log k_5	$pK_A^{HO_2\cdot/O_2\cdot^-}$	log k_2
			Me_2SO		
4-Bromophenol	15.7[b]	≃4.60	20.3	10.6–12.3	4.9–6.0
4-chlorophenol	16.1[c]	4.3. ± 0.06	20.5	10.8–12.5	4.7–5.8
phenol	16.9[c]	3.80 ± 0.09	20.7	11.0–12.7	4.1–5.2
p-cresol	17.2[d]	3.01 ± 0.09	20.2	10.5–12.2	3.3–4.4
2,4-dimethylphenol	17.5[e]	2.52 ± 0.09	20.2	10.5–12.2	2.8–3.9
nitromethane	17.2[f]	2.80 ± 0.3	20.0	10.3–12.0	2.5 ± 0.1[k]
			av: 20.3	av: 10.6–12.3	
			DMF		
phenol	19.8[g]	3.74 ± 0.09	23.5	13.5–15.5	4.0–5.4
p-cresol	20.1[h]	3.48 ± 0.06	23.6	13.6–15.6	3.8–5.2
			av: 23.5_5	av: 13.5_5–15.5_5	

[a] +0.1 M NBu_4BF_4, temperature 25 °C, all rate constants are in $M^{-1}\,s^{-1}$. [b] From ref 15a. [c] From ref 15b. [d] From the pK_As of *p*- and *m*-cresol in water[15d] and the pK_A of *m*-cresol in Me_2SO.[15b] [e] From the pK_As of 2.4-dimethylphenol[15e] and phenol[15d] in water and the pK_A of phenol in Me_2SO.[15b] [f] From ref 15b. [g] From ref 15f. [h] From the pK_A of *p*-cresol and phenol in water[15d] and the pK_A of phenol in DMF.[15f]

DISP1–DISP2, with $k_{-2}/k_5 = 0.5$, in the case of nitromethane, allows the determination of the rate parameter K_2k_5 in all cases and, in addition, of k_2 in the case of nitromethane (Table V). It is then possible to calculate

$$pK_A^{HO_2\cdot/O_2\cdot^-} + \log k_5 = \log K_2k_5 + pK_A^{HA/A^-}$$

Since k_5 has no reason to vary with the acid, this expression should be constant in the series. That this is indeed the case, providing a test of consistency of the data, is seen in Table V.

The driving force of reaction 5 can be estimated as follows. In water, $E_{O_2/O_2\cdot^-} = -0.16$ V vs. NHE[1g] and $E_{HO_2\cdot/HO_2^-} = 0.747$ V vs. NHE,[1g] and thus the driving force of reaction 5 is 0.906 V. In DMF, it can be estimated as equal to 0.938 V.[16] In Me_2SO, the driving force is likely to be of the same order of magnitude. Although the driving force is large, it is not certain that the reaction proceeds at the diffusion limit. Indeed, in water, k_5 is equal to 10^8 $M^{-1}\cdot s^{-1}$,[1,17] i.e., significantly below the diffusion limit. In terms of Marcus theory,[18] the internal reorganization factor should be about the same in water, Me_2SO, and DMF.

The solvent reorganization factors should be larger in water than in Me_2SO and DMF since solvation of $O_2\cdot^-$ and HO_2^- is stronger in the first case than in the second and third. It follows that we can assume that k_5 is comprised between 10^8 and either 5×10^9 or 10^{10} $M^{-1}\cdot s^{-1}$ for Me_2SO and DMF, respectively.[19]

By using this estimation of k_5, it is thus possible to obtain an estimate of the pK_A of the $HO_2\cdot/O_2\cdot^-$ couple as shown in Table V. The values thus obtained are consistent with that in water (4.75).[17] The mean pK_a difference between Me_2SO and water for a series of acids including chloracetic, benzoic, *p*-toluidic, acetic, phenol, and nitromethane is 6.9.[15] A value of 11.7 is thus predicted for the pK_A of the $HO_2\cdot/O_2\cdot^-$ couple in Me_2SO, which falls within our estimation range. This corresponds to $k_5 = 4 \times 10^8$ $M^{-1}\cdot s^{-1}$.

The fact that a DISP2 behavior is observed with all phenols indicates that $k_{-2} \geq 2k_5$ (see Figure 5). On the other hand, k_{-2} cannot overcome the diffusion limit, i.e., for molecules of different sizes like $HO_2\cdot$ and phenols, 10^{10} and 2×10^{10} $M^{-1}\cdot s^{-1}$ in Me_2SO and DMF, respectively. The ratio k_{-2}/k_5 is therefore comprised between 2 and 25 in Me_2SO (50 in DMF). An estimate of the forward proton transfer rate constant ensues as shown in Table V. The question then arises why the situation is different in the case of nitromethane where the kinetic regime is closer to the DISP1 case ($k_{-2}/k_5 = 0.5$) than in the case of phenols where k_{-2}/k_5 is at least equal to 2. A likely reason for this is that the standard rate constant of protonation should be lower for nitromethane than for phenols since the negative charge in the conjugate base is expected to be more localized in the first case than in the latter due to delocalization over the phenyl ring.[20]

Let us finally come back to the reaction mechanism, previously accepted,[5b-d] involving the H-atom disproportionation of two $HO_2\cdot$ radicals (reaction 7). In water, $k_5 = 9 \times 10^7$ and $k_7 = 8 \times 10^5$ $M^{-1}\cdot s^{-1}$. When going to an aprotic solvent, such as Me_2SO or DMF, k_5 is likely to increase as discussed earlier, whereas k_7 should remain about the same since, the reactants and products being uncharged, the solvent reorganization free energy should be small in all solvents. In this context, the reason why reaction 5 predominates over reaction 7 is that the preceding protonation step (reaction 2) is an uphill reaction with an equilibrium constant ranging from 10^{-6} to 10^{-4}. It follows that the reaction of two $HO_2\cdot$ radicals is disfavored as compared to the reaction of $HO_2\cdot$ with $O_2\cdot^-$ by the same very large factor. It is conceivable that by using stronger and stronger acids, reaction 7 could enter into the competition favorably. However, since reaction 2 then becomes more and more rapid from left to right, reaction 3 would, under these conditions, overcome both reactions 5 and 7, giving rise to an ECE mechanism and thus preventing the H-atom exchange disproportionation of $HO_2\cdot$ radicals to be observed.

In closing, let us emphasize that the mechanistic conclusions we have drawn and the rate and equilibrium constants we have determined using the DPSC techniques correspond to homogeneous reactions unperturbed by the electrical double layer[21] and are thus not affected by the fact that the electrons are supplied to the system in a heterogeneous manner.

Experimental Section

Instrumentation and Measuring Procedures. All the experiments were carried out at 25 ± 0.1 °C, using a cell equipped with a jacket allowing circulation of water from a thermostat. Two concentrations of oxygen (2.1 and 0.44 mM in Me_2SO; 4.8 and 1.0 mM in DMF) were used. They were obtained by saturating the solution with pure oxygen and air, respectively.[3e,5a] The working electrode was a 3 mm carbon disk polished with a 1 μm diamond paste before use. The reference electrode was an aqueous SCE. A homebuilt potentiostat equipped with positive feedback compensation[22] was used for the potential step experiments together with

(16) (a) $\log K_5 = \log K_7 - pK_A^{H_2O_2/HO_2^-} + pK_A^{HO_2\cdot/O_2\cdot^-}$. $K_7 = 10^{25}$.[5b] An approximate value of $pK_A^{HO_2\cdot/O_2\cdot^-}$ is 12.[5b] According to ref 16b, $pK_A^{H_2O_2/HO_2^-} = 11$. However, this value seems grossly underestimated. A more reasonable value can be derived from the observation that the pK_A of H_2O_2 is 1.6 units larger[16c] than that of phenol.[16d] From the latter[5b] it follows that $pK_A^{H_2O_2/HO_2^-} = 21$ and thus $\log K_5 = 16$. (b) Nanni, E. J.; Stallings, M. D.; Sawyer, D. T. *J. Am. Chem. Soc.* **1980**, *102*, 4481. (c) Anne, A., Thèse, Paris, 1985, p 35. (d) Barrette, W. C.; Johnson, H. W.; Sawyer, D. T. *Anal. Chem.* **1984**, *56*, 1890. (e) The distance between the pK_A's of H_2O_2 and phenol is likely to be of the same order of magnitude in Me_2SO. This and the fact that the acid is in excess over O_2 in our experiments is a justification of the assumption we have made above in treating the DISP2 and DISP1–DISP2 kinetics, that reaction 4 is irreversible from left to right.

(17) Bielski, B. H. J.; Allen, A. O. *J. Phys. Chem.* **1977**, *81*, 1048.

(18) Marcus, R. A.; Sutin, N. *Biophys. Biochim. Acta* **1985**, *811*, 265.

(19) Andrieux, C. P.; Blocman, C.; Dumas-Bouchiat, J. M.; M'Halla, F.; Savéant, J. M. *J. Am. Chem. Soc.* **1980**, *102*, 3806.

(20) (a) A related observation is that the solvent reorganization free energy for electron transfer is larger in the case in aliphatic nitro compounds than in the case of aromatic compounds in similar solvents (DMF, acetonitrile).[19b] (b) Savéant, J. M.; Tessier, D. *Faraday Discuss. Chem. Soc.* **1982**, *74*, 57.

(21) (a) Under our conditions, the double layer is about 10^{-7} cm thick whereas the reaction layer is at miminum 10^{-4} cm thick, i.e., 1000 times larger.[2,20b] (b) Savéant, J. M. *J. Electroanal. Chem.* **1980**, *112*, 175; **1983**, *143*, 447.

(22) Garreau, D.; Savéant, J. M. *J. Electroanal. Chem.* **1972**, *35*, 309.

a PAR 175 Universal Programmer function generator. The current was recorded by means of a homebuilt acquisition device controlled by an Apple II microcomputer. The potential was stepped from −0.1 to −1.2 V vs. SCE in Me_2SO and from −0.15 to −1.4 V vs. SCE in DMF, so as to avoid the reoxidation of the conjugate base of the acid. Electrolysis of O_2 in Me_2SO was carried out at a 30 cm^2 carbon electrode. H_2O_2 was titrated according to the method described in ref 7b and 23.

Chemicals. Me_2SO of pharmaceutical grade was used after reduced pressure distillation and recrystallization. DMF was vacuum distilled before used. NBu_4BF_4 (Fluka, puriss.) was used as supporting electrolyte. All the other chemicals were from commercial origin and were used as received.

Formal Kinetics. Mechanism involving H-atom transfer from the solvent to the $HO_2^\bullet$ radicals:

$$O_2 + e^- \rightleftarrows O_2^{\bullet -} \quad (1)$$

$$O_2^{\bullet -} + HA \underset{k_{-2}}{\overset{k_2}{\rightleftarrows}} HO_2^\bullet + A^- \quad (2)$$

$$HO_2^\bullet + CH_3SOCH_3 \xrightarrow{k_6} H_2O_2 + {}^\bullet CH_2SOCH_3 \quad (6)$$

$${}^\bullet CH_2SOCH_3 + e^- \rightleftarrows {}^-CH_2SOCH_3 \quad (8)$$

or

$${}^\bullet CH_2SOCH_3 + O_2^{\bullet -} \rightarrow {}^-CH_2SOCH_3 + O_2 \quad (8')$$

$${}^-CH_2SOCH_3 + HA \rightarrow CH_3SOCH_3 + A^- \quad (9)$$

If the production of $HO_2^\bullet$ through reaction 2 is fast, the mechanism will take place within an ECE context, involving the reaction sequence (1) + (2) + (6) + (8) + (9). Conversely, when the production of $HO_2^\bullet$ is slow, reaction 8′ will predominate over reaction 8, thus giving rise to a DISP-type mechanism ((1) + (2) + (6) + (8′) + (9)).

Introducing the dimensionless variables and parameters $a = [O_2]/C^\circ$, $b = [O_2^{\bullet -}]/C^\circ$, $c = [HO_2^\bullet]/C^\circ$, $r = [{}^\bullet CH_2SOCH_3]/C^\circ$, $s = [{}^-CH_2SOCH_3]/C^\circ$, $w = [A^-]/C^\circ$, $\tau = t/\theta$, $y = x(D\theta)^{-1/2}$, $\psi = i\theta^{1/2}/FSC^\circ D^{1/2}$, $\lambda_2 = k_2 C^\circ_{HA}\theta$, $\lambda_{-2} = k_{-2}C^\circ\theta$, $\lambda_6 = k_6 C^\circ\theta$, $\lambda'_8 = k_8' C^\circ\theta$ (C°, C°_{HA} bulk concentrations of O_2 and HA, respectively, t = time, θ = inversion time of the potential step, x = distance from the electrode surface, D = mean value of the diffusion coefficient of the various species, i = current, S = electrode surface area), the current function, ψ, is obtained from the resolution of the following set of partial derivative equations, boundary, and initial conditions deriving from the second Fick law, modified by the appropriate kinetic terms, as applied to each species the concentration of which is not negligible and from the steady state assumption as applied to $HO_2^\bullet$ in both the ECE and the DISP regimes and, in addition to ${}^\bullet CH_2SOCH_3$ and ${}^-CH_2SOCH_3$ in the DISP regime.

ECE	DISP
$\frac{\partial a}{\partial \tau} = \frac{\partial^2 a}{\partial y^2}$	$\frac{\partial^2 2a + b}{\partial \tau} = \frac{\partial^2 2a + b}{\partial y^2}$
$\frac{\partial b}{\partial \tau} = \frac{\partial^2 b}{\partial y^2} - \frac{\lambda_2\lambda_6 b}{\lambda_{-2}w + \lambda_6}$	$\frac{\partial b}{\partial \tau} = \frac{\partial^2 b}{\partial y^2} - \frac{2\lambda_2\lambda_6 b}{\lambda_{-2}w + \lambda_6}$
$\frac{\partial b + r}{\partial \tau} = \frac{\partial^2 b + r}{\partial y^2}$	$\frac{\partial b + w}{\partial \tau} = \frac{\partial^2 b + w}{\partial y^2}$
$\frac{\partial b + s + w}{\partial \tau} = \frac{\partial^2 b + s + w}{\partial y^2}$	

$\tau = 0, y > 0$ and $y = \infty, \tau > 0$: $a = 1, b = r = s = w = 0$

$y = 0, \tau > 0$: $\frac{\partial a}{\partial y} + \frac{\partial b}{\partial y} = 0, \frac{\partial r}{\partial y} + \frac{\partial s}{\partial y} = 0, \frac{\partial w}{\partial y} = 0, a = 0, r = 0$

$$\psi = \left(\frac{\partial a}{\partial y}\right)_0 + \left(\frac{\partial s}{\partial y}\right)_0 \qquad \psi = \left(\frac{\partial a}{\partial y}\right)_0$$

In both regimes, there are two limiting cases according to the value of the parameter λ_{-2}/λ_6:

(1) If $\lambda_{-2}/\lambda_6 \rightarrow 0$, i.e., if forward relation 2 is the rate-determining step of reaction 2 and 6, the ψ function and thus R depends upon the parameter $\lambda_2 = k_2 C^\circ_{HA}\theta$ and we obtained the ECE_{irr} case and the DISP1 case, respectively, since the equations are then the same as in these two cases.[7a]

(2) If $\lambda_{-2}/\lambda_6 \rightarrow \infty$, i.e., if reaction 2 acts as a preequilibrium for the rate-determining step, the kinetic term in the b equation becomes $(\lambda_2\lambda_6/\lambda_{-2})(b/w)$. R is, in both cases, a function of the parameter $(k_2k_6/k_{-2})C^\circ_{HA}/C^\circ$. We thus obtain the two limiting situations that have been denoted ECE'_{irr} and DISP3, respectively. The corresponding R vs. $(\lambda_2\lambda_6/\lambda_{-2})$ working curves can be computed in each case by numerical finite difference resolution of the above set of equations. What is more important for the present purposes is the resulting values of $\gamma(-1)$ and $\delta(1)$.

Mechanism involving the H-atom disproportionation of two $HO_2^{\bullet -}$ radicals:

$$O_2 + e^- \rightleftarrows O_2^{\bullet -} \quad (1)$$

$$O_2^{\bullet -} + HA \underset{k_{-2}}{\overset{k_2}{\rightleftarrows}} HO_2^\bullet + A^- \quad (2)$$

$$2HO_2^\bullet \xrightarrow{k_7} H_2O_2 + O_2 \quad (7)$$

With the same transformations and notations as above (in addition, $\lambda_7 = k_7 C^\circ\theta$), the problem is described by the following dimensionless formulation

$$\frac{\partial 2a + b}{\partial \tau} = \frac{\partial^2 2a + b}{\partial y^2}, \frac{\partial b}{\partial \tau} = \frac{\partial^2 b}{\partial y^2} - 2\lambda_7 c^2, \frac{\partial b + w}{\partial \tau} = \frac{\partial^2 b + w}{\partial y^2}$$

$\tau = 0, y > 0$ and $y = \infty, \tau > 0$: $a = 1, b = w = 0$

$y = 0, \tau > 0$: $\frac{\partial a}{\partial y} + \frac{\partial b}{\partial y} = 0, \frac{\partial w}{\partial y} = 0, a = 0$

$$\psi = (\partial a/\partial y)_0$$

The steady-state assumption was applied to $HO_2^\bullet$ leads to

$$c = \frac{\lambda_2 b}{2\lambda_7 c + \lambda_{-2}w}$$

There are thus two limiting cases according to the value of λ_{-2}/λ_7.

(1) If $\lambda_{-2}/\lambda_7 \rightarrow 0$ (reaction 2 is the rate-determining step)

$$\frac{\partial b}{\partial \tau} = \frac{\partial^2 b}{\partial y^2} - \lambda_2 b$$

The kinetics are the same as for DISP1 leading the values of γ and δ reported in Table I.

(2) If $\lambda_{-2}/\lambda_7 \rightarrow \infty$ (reaction 7 is the rate-determining step with reaction 2 as a preequilibrium)

$$\frac{\partial b}{\partial \tau} = \frac{\partial^2 b}{\partial y^2} - \frac{2\lambda_7\lambda_2^2}{\lambda_{-2}^2}\frac{b^2}{w^2}$$

The R vs. $\lambda_7\lambda_2^2/\lambda_{-2}^2$ working curve can be computed from numerical resolution of the above equation in this case that we have denoted DISP4. What is more important for our discussion is that R is a function of the kinetic parameter

$$\left(\frac{\lambda_2}{\lambda_{-2}}\right)^2\lambda_7 = \left(\frac{k_2}{k_{-2}}\right)^2 k_7 \frac{C^\circ_{HA}{}^2}{C^\circ_{O_2}}\theta$$

thus leading to the values of γ and δ reported in Table I.

Mechanism involving the electron transfer reduction of $HO_2^\bullet$ by $O_2^{\bullet -}$. Competition between the DISP1 and DISP2 pathways. The data found with nitromethane appear to fall in between the DISP1 and DISP2 cases, i.e., in the reaction sequence

$$O_2 + e^- \rightleftarrows O_2^{\bullet -} \quad (1)$$

$$O_2^{\bullet -} + HA \underset{k_{-2}}{\overset{k_2}{\rightleftarrows}} HO_2^\bullet + A^- \quad (2)$$

$$HO_2^\bullet + O_2^{\bullet -} \xrightarrow{k_5} HO_2^- + O_2 \quad (5)$$

$$HO_2^- + HA \rightarrow H_2O_2 + A^- \quad (4)$$

both reactions 2 and 5 participate in the rate control. With the same transformations and notations as above (in addition, $\lambda_5 = k_5 C^\circ\theta$) the

(23) Charlot, G. *Chimie Analytique Quantitative*; Masson: Paris, 1974; Vol. 2, pp 474 and 545.

(24) Crank, J. *Mathematic of Diffusion*; Clarendon Press: Oxford, 1964.

following dimensionless formulation is obtained, noting that the steady-state approximation is applied to $HO_2^{\bullet}$ and HO_2^-

$$\frac{\partial 2a+b}{\partial \tau} = \frac{\partial^2 2a+b}{\partial y^2}, \quad \frac{\partial b}{\partial \tau} = \frac{\partial^2 b}{\partial y^2} - \frac{2\lambda_2 b^2}{b + \frac{\lambda_{-2}}{\lambda_5} w}, \quad \frac{\partial b+w}{\partial \tau} = \frac{\partial^2 b+w}{\partial y^2}$$

$$\tau = 0,\ y > 0 \text{ and } y = \infty,\ \tau > 0:\ a = 1,\ b = w = 0$$

$$y = 0,\ \tau > 0:\ \frac{\partial a}{\partial y} + \frac{\partial b}{\partial y} = 0,\ \frac{\partial w}{\partial y} = 0,\ a = 0$$

$$\psi = (\partial a/\partial y)_0$$

The system thus depends upon two parameters that can be chosen either as λ_2 and λ_{-2}/λ_5 or as $(\lambda_2/\lambda_{-2})\lambda_5$ and λ_{-2}/λ_5.

If $\lambda_{-2}/\lambda_5 \to 0$, the rate-determining step is reaction 2, we obtain the DISP1 behavior, and R is then a function of λ_2. Conversely, if $\lambda_{-2}/\lambda_5 \to \infty$, the rate-determining step is reaction 5, reaction 2 being a pree-quilibrium, we obtain the DISP2 behavior. For intermediate values of the parameter λ_{-2}/λ_5 ($=k_{-2}/k_5$), the working curves were computed by an explicit finite difference[23] resolution of the above system. The results are shown in Figure 5 under the form of R vs. λ_2 (Figure 5a) and R vs. $\lambda_2\lambda_5/\lambda_{-2}$ (Figure 5b) working curves for a series of values of the competition parameter k_{-2}/k_5. In order to apply the finite difference technique to only the two last partial derivation equations, the first one was integrated formally leading to

$$b_0 = 2 - \pi^{-1/2} \int_0^{\tau} \psi(\eta)(\tau - \eta)^{-1/2}\, d\eta$$

Conclusions

The main conclusions emerging from the above results and discussion concern the chemical reactivity of the $O_2^{\bullet-}$ and $HO_2^{\bullet}$ radicals generated from the electrochemical generation of the former in the presence of acids. In aprotic solvents, the $HO_2^{\bullet}$ radical appears as an electron transfer oxidant toward $O_2^{\bullet-}$ rather than an H-atom abstractor from the solvent or from another $HO_2^{\bullet}$ radical. $O_2^{\bullet-}$ displays both weak base and weak electron-transfer reductant properties. In neutral and moderately acidic media, the mechanism of superoxide ion disproportionation in aprotic solvents such as Me_2SO and DMF appears to be quite similar to what it is in water[17] involving, after protonation into the $HO_2^{\bullet}$, electron transfer to $HO_2^{\bullet}$ from $O_2^{\bullet-}$.

Acknowledgment. We thank Dr. K. B. Su for his help in applying the fitting procedures.

Registry No. O_2, 7782-44-7; $O_2^{\bullet-}$, 11062-77-4; $HO_2^{\bullet}$, 3170-83-0; phenol, 108-95-2; *p*-cresol, 106-44-5; 4-bromophenol, 106-41-2; 4-chlorophenol, 106-48-9; 2,4-dimethylphenol, 105-67-9; nitromethane, 75-52-5.

Communications to the Editor

Isolation and X-ray Crystal Structure of the Tetrameric Lithium-Coordinated α-Sulfonimidoyl Carbanion $[(Me_3Si)CH\{S(O)(NSiMe_3)\}Li]_4$: The First Structure of an α-SO Substituted Lithium Alkyl Having No External Donor Ligands

Hans-Joachim Gais* and Uwe Dingerdissen[1]

Chemisches Laboratorium der Albert-Ludwigs-Universität Institut für Organische Chemie und Biochemie D-7800 Freiburg i. Br., West Germany

Carl Krüger and Klaus Angermund

Max-Planck-Institut für Kohlenforschung D-4330 Mülheim 1, West Germany

Received November 28, 1986

The chiral lithium alkyl sulfoximides **1** have been established as useful intermediates in asymmetric synthesis.[2] For a deeper understanding of the factors determining the reactivity of **1**, e.g., in asymmetric bond formation[2a,b] and elimination[2c] reactions, knowledge of their structure is a prerequisite. Up till 1986, however, definitive structural information about **1** was completely lacking. Recently we described an X-ray crystal structure analysis

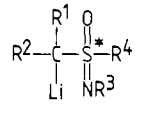

1a, $R^1 = R^2 = H$, $R^3 = Me$, $R^4 = Ph$
1b, $R^1 = H$, $R^2 = R^3 = SiMe_3$, $R^4 = Ph$

of the tetramethylethylenediamine (tmeda)-complexed (*S*)-(*N*-methyl-*S*-phenylsulfonimidoyl)methyllithium (**1a**),[3] which revealed a chiral tetramer, $(\mathbf{1a})_4 \cdot (tmeda)_2$, of approximately C_2 symmetry, with short bonds between the anionic C atoms and the sulfonimidoyl groups [mean value of C–S distance, 1.64 (2) Å], similar to those found in lithium alkyl sulfones,[4] and two different kinds of Li and anionic C atoms, respectively. Whereas two of the latter have a C–Li bond [mean value of C–Li distance, 2.49 (5) Å], the others are only weakly, if at all, coordinated, each to two Li atoms [mean value of C–Li distance, 3.23 (4) Å]. However, the strongly chelating tmeda ligands should undoubtedly play a significant role in the structure of $(\mathbf{1a})_4 \cdot (tmeda)_2$, and the alteration brought about by the donor ligands was an open question. We now report the X-ray crystal structure of the (trimethylsilyl)[*N*-(trimethylsilyl)-*S*-phenylsulfonimidoyl]methyllithium tetramer $(\mathbf{1b})_4$ having no external donor ligands and first results about its solution structure. The two trimethylsilyl groups were deliberately chosen, among other reasons, to achieve sufficient solubility of **1b** in noncomplexing solvents, allowing not only crystal growing but also NMR investigations therein. **1b** which carries two different substituents at the anionic C atom was generated from (±)-trimethyl[(*N*-(trimethylsilyl)-*S*-phenylsulfonimidoyl)methyl]silane (**2**)[5] with 1 equiv of *n*-butyllithium in *n*-hexane at -30 °C. Clear colorless crystals which are *readily soluble in cyclohexane as well as tetrahydrofuran* (THF) were slowly grown from a 4:1 cyclohexane/*n*-hexane mixture at room temperature. The X-ray

(1) Present address: Institut für Chemische Technologie, Technische Hochschule, D-6100 Darmstadt, Germany.

(2) (a) Johnson, C. R.; Zeller, J. R. *Tetrahedron* **1984**, *40*, 1225. (b) Johnson, C. R. *Aldrichim. Acta* **1985**, *18*, 3. (c) Erdelmeier, I.; Gais, H.-J.; Lindner, H. J. *Angew. Chem., Int. Ed. Engl.* **1986**, *25*, 935.

(3) Gais, H.-J.; Erdelmeier, I.; Lindner, H. J.; Vollhardt, J. *Angew. Chem., Int. Ed. Engl.* **1986**, *25*, 938.

(4) (a) $[(CH_2SO_2Ph)Li \cdot tmeda]_2$: Gais, H.-J.; Lindner, H. J.; Vollhardt, J. *Angew. Chem., Int. Ed. Engl.* **1985**, *24*, 859. (b) $[(PhCHSO_2Ph)Li \cdot tmeda]_2$: Boche, G.; Marsch, M.; Harms, K.; Sheldrick, G. M. *Angew. Chem., Int. Ed. Engl.* **1985**, *24*, 573. (c) $[(CH_2{=}CHCHSO_2Ph)Li \cdot diglyme]_2$: Gais, H.-J.; Vollhardt, J.; Lindner, H. J. *Angew. Chem., Int. Ed. Engl.* **1986**, *25*, 939.

(5) For synthesis, see: Dingerdissen, U. Diploma Thesis, Technische Hochschule Darmstadt 1985.

0002-7863/87/1509-3775$01.50/0